

A FREE-STANDING PAN/PMMA/rGO CARBON PAPER AS AN EFFECTIVE INTERLAYER FOR HIGH PERFORMANCE LITHIUM-SULFUR BATTERIES

by

Ya LI^{a*}, Leigen LIU^{b*}, Zhenfeng LIN^c, and Shao-Wen YAO^{d*}

^a College of Textile Science and Engineering (International College of Silk), Zhejiang Sci-Tech University, Hangzhou, Zhejiang, China

^b School of Art and Textile and Clothing Engineering, Changshu Institute of Technology, Changshu, China

^c Sujing Environmental Protection New Materials Co., Ltd., Suzhou, China

^d School of Mathematics and Information Science, Henan Polytechnic University, Jiaozuo, China

Original scientific paper
<https://doi.org/10.2298/TSCI2004485L>

The limitations of the polysulfides shuttling and lithium dendrites have been obstacles to improve the lithium-sulfur battery technology, resulting in low active material utilization and poor cycle life. Here we report a simple modification of the traditional lithium-sulfur battery configuration to achieve high capacity with a long cycle life and high reversible rate. Great improvement was observed with a carbonized PAN/PMMA/rGO paper between the anode and the separator in the active material utilization and capacity retention. The adding of a free-standing PAN/PMMA/rGO carbon interlayer demonstrated the feasibility of enhancing the performance of lithium-sulfur batteries.

Key words: PAN/PMMA/rGO carbon paper, interlayer, lithium-sulfur battery, performance

Introduction

With the continuously increasing demand of energy consumption, lithium-sulfur (Li-S) battery has been catching increasing attention, because it is low cost, environmentally friendly and has high theoretical specific capacity of as high as 1675 mAh/g, great energy density of as high as 2500 Wh/kg [1, 2]. However, practical applications of the Li-S batteries have been hindered by some inherent limitations, such as low active material utilization, short cycle life and severe self-discharge. The reasons for these obstructed elements are the insulating properties of sulfur and its intermediates, the large volume change during the intercalation process and the polysulfide shuttle effects [3].

Much research work has been made to resolve these issues normally by physical confinement of cathode. Sulfur was mixed with all kinds of carbons [4-6], oxides [7-9], conductive polymer coating [10, 11] through binders to augment conductivity. They have showed good results on preventing the dissolution of polysulfides. Besides, a separator is also a necessary component in the battery as it separates the cathode from the anode from the cathode to serve as the electrolyte reservoir to help the transport of ions [12]. Therefore, another alterna-

* Corresponding author, e-mail: liya@zstu.edu.cn; liuleiyin@aliyun.com; ysw140917@163.com

tive and simple strategy to prevent polysulfides transferring is to develop a modified functional separator [13]. Inserting a carbon interlayer between the sulfur cathode and separator had unique advantages of improving the performance of Li-S batteries [14-19]. Thus, the interlayer was proved to minimize the diffusion of lithium polysulfides and promote the utilization of active materials, and the cycle performance could be improved.

Among the interlayers, carbonized electrospun nanofibers have received attention owing to their highly porous structure, controllable thickness and good electrolyte wettability, which can ensure the fast transfer of ions [20]. Even though the principle of electrospinning continues to be explored [21-36], needle electrospinning remains the most basic method for producing high quality nanofibers. In order to promote the cyclic stability and maintain the energy density advantage of Li-S batteries, herein, we present a PAN/PMMA/rGO carbon paper fabricated by electrospinning after thermal treatment as the interlayer. Its bifunctional role toward the protection of both anode and cathode is explored. By introducing the carbonized PAN/PMMA/rGO interlayer, we compare it with the pure Celgard PP separator in the Li-S battery, the limited soluble polysulfides loss ratio is expected, which not only reduces the electrochemical resistance but also localizes the migrating polysulfides and traps them, thereby improving the discharge capacity as well as cyclability.

Experimental

For the preparation of PAN/PMMA/rGO solution, 0.3 g reduced graphene oxide (rGO) was first dispersed in 27.6 g Dimethylformamide (DMF) solvent under sonication. PAN/PMMA (7:3 by quality) was then added to the rGO-dispersed solution and stirred overnight to form a homogenous 8 wt.% solution. The as-spun nanofiber membrane was collected on an aluminum plate with a flow rate of 0.75 mL/h at a high voltage of 15 kV and the tip-to-collector was set at 15 cm. The thickness of the PAN/PMMA/rGO nanofiber was fixed at $70 \pm 5 \mu\text{m}$. The as-prepared nanofiber mat was stabilized in air at 250 °C for 2.5 hours with a heating rate of 5 °C min⁻¹, and then treated in nitrogen at 800 °C for 2 hours with a heating rate of 2 °C min⁻¹ to obtain the carbonized PAN/PMMA/rGO paper. Schematic illustration of the fabrication process of the interlayer is shown in fig. 1(a), respectively.

The electrolyte was prepared by dissolving 1 M LiTFSI and 0.1 M lithium nitrite in a mixture of DOL and DME (1:1 by volume). The carbon-coated aluminum foil containing 70 wt.% pure sulfur, 20 wt.% TIMCAL, and 10 wt.% PVDF was made as cathode, whose sulfur loading was from 0.8 to 2.0 mg/cm, then it was put in a vacuum oven at 60 °C overnight. Testing cells (2032-type) were assembled by the sulfur electrodes, celgard PP separators, PAN/PMMA/rGO carbon paper interlayer and Li metal as the anode in an argon-filled glove box. The schematic configurations of Li-S cells with bare PP separator as control sample and a bifunctional interlayer were displayed in figs. 1(b) and 1(c), respectively. The cells were charged and discharged between 1.7 and 2.8 V on a battery tester at room temperature. The cyclic voltammetry (CV) was conducted at a scan rate of 0.1 mV/s.

Results and discussion

Here, to test the properties of the PAN/PMMA/rGO as an interlayer in Li-S batteries, coin cells were assembled with or without the interlayer. The CV of the cells were shown in fig. 2 at a scan rate of 0.1 mV/s between 1.7 V and 2.8 V. All CV had two cathodic peaks because of the conversion of sulfur and polysulfides. The cell without interlayer showed the delayed reaction (larger polarization) because of a higher kinetic barrier. It means the adding of the interlayer could suppress the reduction of polysulfides to sulfides. The anodic peaks

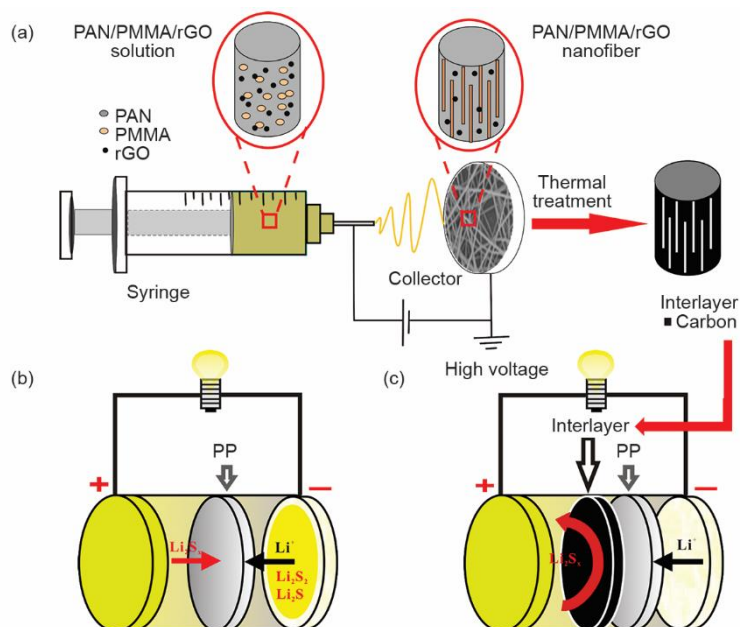


Figure 1. (a) Schematic illustration of the fabrication process of the PAN/PMMA/rGO carbon interlayer, a schematic cell configuration of rechargeable Li-S batteries, (b) traditional configuration with PP separator and (c) new configuration with the interlayer

around 2.3 V were caused by the reversible conversion reaction of insoluble $\text{Li}_2\text{S}_2/\text{Li}_2\text{S}$ to lithium intermediates and further to S_8 . Similarly, the anodic voltage for the cells without interlayer were also slightly higher than those with interlayer. From the comparison, it was obvious that the loop area of the cell without interlayer was smaller. Therefore, the PAN/PMMA/rGO interlayer could enhance the electrochemical stability.

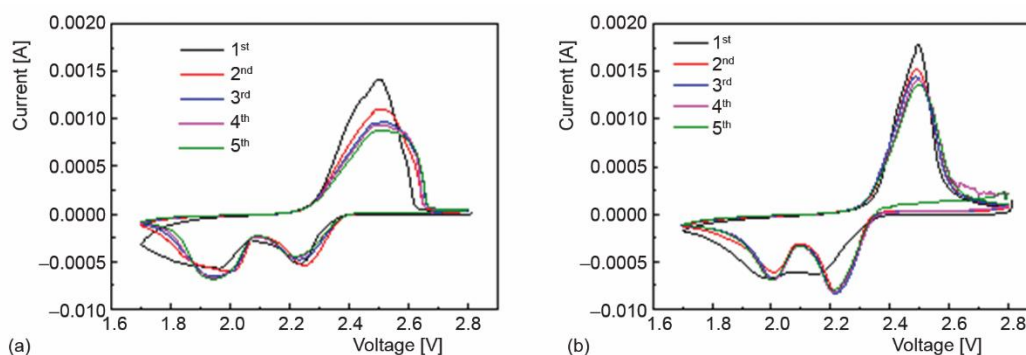


Figure 2. Cyclic voltammogram scans of the Li-S cell (a) without and (b) with interlayer at a potential sweep rate of 0.1 mV/s

To manifest the advantageous electrochemical properties of the cell with the PAN/PMMA/rGO interlayer compared with the pure routine PP separator, cycle performance tests for the first 100 cycles at 0.1 C were illustrated in fig. 3. It can be seen that the initial

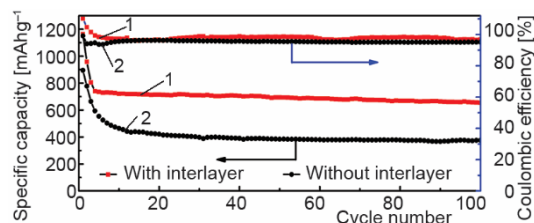


Figure 3. Cycle performance and coulombic efficiency of Li-S cells with routine separator and the PAN/PMMA/rGO carbon interlayer at the current of 335 mA/g; 1 – without interlayer, 2 – with interlayer

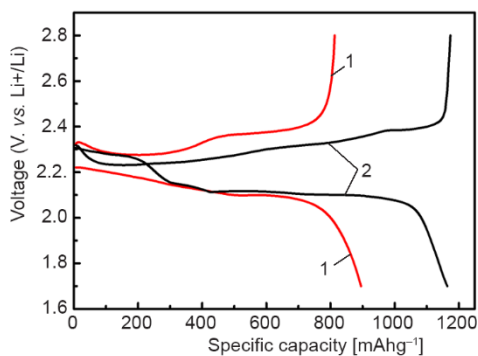


Figure 4. Charge-discharge profiles of the first cycle with and without the PAN/PMMA/rGO carbon interlayer; 1 – without interlayer, 2 – with interlayer

discharge capacity of the cell with and without the interlayer is 1164 mAh/g and 895 mAh/g, respectively. The coulombic efficiency of the cell with the interlayer was higher than the cell using routine separator in the most cycles, which can be attributed to the blocking effect of the carbonized PAN/PMMA/rGO interlayer to the polysulfides and the surface morphology of lithium anode could be stabilized.

The first discharge and charge potential profiles of the cells with and without interlayer were presented in fig. 4. There were two potential plateaus showing at around 2.2 V and 2.1 V during the discharge process, and the charge plateaus were located at about 2.3-2.4 V. Nevertheless, it can also be demonstrated that the cell with the interlayer had higher capacity than that with PP separator and the active materials were utilized more adequately.

Conclusion

The PAN/PMMA/rGO carbon interlayer was prepared from electrospinning with thermal treatment, which could anchor the soluble polysulfides, then the effective confinement minimized the side reaction on the anode side. As a result, after inserting the interlayer,

the utilization of the active materials was improved, high capacities and high Coulombic efficiencies were obtained compared with the pure PP as the routine separator. Therefore, the PAN/PMMA/rGO carbon interlayer improved the performance of the Li-S batteries by stabilizing the surface morphology of lithium anode and confining the polysulfides shuttling.

Acknowledgment

The work is supported by Excellent Ph. D. Program of Zhejiang Sci-Tech University (Grant No. 11110231281803), Scientific Research Foundation of Zhejiang Sci-Tech University (Grant No. 11112932618215) and Science and Technology Project of Jiangsu Province and Suzhou City in China (BE2017676, SS201725, SYG201827).

References

- [1] Yang, Y., et al., Nanostructured Sulfur Cathodes, *Chem. Soc. Rev.*, 42 (2013), 7, pp. 3018-3032
- [2] Zhang, S. S., Liquid Electrolyte Lithium/Sulfur Battery: Fundamental Chemistry, Problems, and Solutions, *J. Power Sources*, 231 (2013), June, pp. 153-162
- [3] Gao, T. J., et al., Effects of Electrospun Carbon Nanofibers' Interlayers on High-Performance Lithium-Sulfur Batteries. *Materials*, 10 (2017), 4, 376
- [4] Ji, X. L., et al., A Highly Ordered Nanostructured Carbon-Sulphur Cathode for Lithium-Sulphur Batteries, *Nat. Mater.*, 8 (2009), 6, pp. 500-506

- [5] Jayaprakash, N., et al., Porous Hollow Carbon@Sulfur Composites for High-Power Lithium-Sulfur Batteries, *Angew. Chem., Int. Ed.*, 50 (2011), 26, pp. 5904-5908
- [6] Yuan, L. X., et al., Improvement of Cycle Property of Sulfur-Coated Multi-walled Carbon Nanotubes Composite Cathode for Lithium/Sulfur Batteries, *J. Power Sources*, 189 (2009), 2, pp. 1141-1146
- [7] Wei, S., et al., Sulphur-TiO₂ Yolk-Shell Nanoarchitecture with Internal Void Space for Long-Cycle Lithium-Sulphur Batteries. *Nat. Commun.*, 4 (2013), 1, pp. 1-6
- [8] Ponraj, R., et al., Improvement of Cycling Performance of Lithium-Sulfur Batteries by Using Magnesium Oxide as a Functional Additive for Trapping Lithium Polysulfide, *ACS Appl. Mater. Interfaces*, 8 (2016), 6, pp. 4000-4006
- [9] Liang, X., et al., A Highly Efficient Polysulfide Mediator for Lithium-Sulfur Batteries, *Nat. Commun.*, 6 (2015), 1, pp. 1-8
- [10] Li, G. C., et al., A Polyaniline-Coated Sulfur/Carbon Composite with an Enhanced High-Rate Capability as a Cathode Material for Lithium/Sulfur Batteries, *Adv. Energy Mater.*, 2 (2012), 10, pp. 1238-1245
- [11] Zhou, W. D., et al., Yolk-Shell Structure of Polyaniline-Coated Sulfur for Lithium-Sulfur Batteries. *J. Am. Chem. Soc.*, 135 (2013), 44, pp. 16736-16743
- [12] Wu, B., et al., Enhanced Cycling Stability of Sulfur Cathode Surface-Modified By Poly (n-methylpyrrole), *Electrochim Acta*, 135 (2014), July, pp. 108-113
- [13] Li, Y., et al., Ultrafine and Polar ZrO₂-Inlaid Porous Nitrogen-Doped Carbon Nanofiber as Efficient Polysulfide Absorbent for High-performance Lithium-Sulfur Batteries with Long Lifespan, *Chem. Eng. J.*, 349 (2018), Oct., pp. 376-387
- [14] Su, Y. S., et al., Lithium-Sulphur Batteries with a Microporous Carbon Paper as a Bifunctional Interlayer, *Nat. Commun.*, 3 (2012), 1, pp. 1-6
- [15] Zhou, G. M., et al., A Graphene-Pure-Sulfur Sandwich Structure for Ultrafast, Long-Life Lithium-Sulfur Batteries, *Adv. Mater.* 26 (2014), 4, pp. 625-631
- [16] Xing, L. B., et al., Nitrogen, Sulfur-Codoped Graphene Sponge as Electroactive Carbon Interlayer for High-Energy and -Power Lithium-Sulfur Batteries, *J. Power Sources*, 303 (2016), Jan., pp. 22-28
- [17] Wei, H., et al., Enhanced Cycle Performance of Lithium-Sulfur Batteries Using a Separator Modified with a PVDF-C Layer, *ACS Appl. Mater. Interfaces*, 6 (2014), 22, pp. 20276-20281
- [18] Singhal, R., et al., A FreeStanding Carbon Nanofiber Interlayer for High-Performance Lithium-Sulfur batteries, *J. Mater. Chem. A*, 3 (2015), 8, pp. 4530-4538
- [19] Balach, J., et al., Mesoporous Carbon Interlayers with Tailored Pore Volume as Polysulfide Reservoir for High-Energy Lithium-Sulfur Batteries, *J. Phys. Chem. C*, 119 (2015), 9, pp. 4580-4587
- [20] Xue, J., et al., Electrospinning and Electrospun Nanofibers: Methods, Materials, and Applications, *Chem. Rev.*, 119 (2019), 8, pp. 5298-5415
- [21] Yu, D. N., et al., Snail-based nanofibers, *Materials Letters*, 220 (2018), 1, pp. 5-7
- [22] Li, X. X., He, J. H., Nanoscale Adhesion and Attachment Oscillation Under the Geometric Potential, Part 1: The formation Mechanism of Nanofiber Membrane in the Electrospinning, *Results in Physics*, 12 (2019), Mar., pp. 1405-1410
- [23] Liu, Y. Q., et al., Nanoscale Multi-Phase Flow and Its Application to Control Nanofiber diameter, *Thermal Science*, 22 (2018), 1, pp. 43-46
- [24] He, J. H., et al., Review on Fiber Morphology Obtained by the Bubble Electrospinning and Blown Bubble Spinning, *Thermal Science*, 16 (2012), 5, pp. 1263-1279
- [25] Zhao, L., et al., Sudden Solvent Evaporation in Bubble Electrospinning for Fabrication of Unsmooth Nanofibers, *Thermal Science*, 21 (2017), 4, pp. 1827-1832
- [26] Liu, L. G., et al., Solvent Evaporation in a Binary Solvent System for Controllable Fabrication of Porous Fibers by Electrospinning, *Thermal Science*, 21 (2017), 4, pp. 1821-1825
- [27] Tian, D., et al., Self-Assembly of Macromolecules in a Long and Narrow Tube, *Thermal Science*, 22 (2018), 4, pp. 1659-1664
- [28] Peng, N. B., et al., A Rachford-Rice Like Equation for Solvent Evaporation in the Bubble Electrospinning, *Thermal Science*, 22 (2018), 4, pp. 1679-1683
- [29] Liu, Z., et al., A Mathematical Model for the Formation of Beaded Fibers in Electrospinning, *Thermal Science*, 19 (2015), 4, pp. 1151-1154
- [30] Tian, D., et al., Macromolecular Electrospinning: Basic Concept & Preliminary Experiment, *Results in Physics*, 11 (2018), Dec., pp. 740-742
- [31] Li, X. X., et al., The Effect of Sonic Vibration on Electrospun Fiber Mats, *Journal of Low Frequency Noise, Vibration and Active Control*, 38 (2019), 3-4, pp. 1246-1291

- [32] Tian, D., *et al.*, Geometrical Potential and Nanofiber Membrane's Highly Selective Adsorption Property, *Adsorption Science & Technology*, 37 (2019), 5-6, pp. 367-388
- [33] Liu, L. G., *et al.*, Electrospun Polysulfone/Poly (Lactic Acid) Nanoporous Fibrous Mats for Oil Removal from Water, *Adsorption Science & Technology*, 37 (2019), 5-6, pp. 438-450
- [34] Li, Y., *et al.*, Fabrication and Characterization of ZrO₂ Nanofibers by Critical Bubble Electrospinning for High-Temperature-Resistant Adsorption and Separation, *Adsorption Science & Technology*, 37 (2019), 5-6, pp. 425-437
- [35] Zhou, C. J., *et al.*, Silkworm-Based Silk Fibers by Electrospinning, *Results in Physics*, 15 (2019), Dec., ID 102646
- [36] Zhao, J. H., *et al.*, Needle's Vibration in Needle-Disk Electrospinning Process: Theoretical Model and Experimental Verification, *Journal of Low Frequency Noise, Vibration and Active Control*, 38 (2019) 3-4, pp. 1338-1344